catalysts

MDPI

Article

Novel Allyl Cobalt Phosphine Complexes: Synthesis, Characterization and Behavior in the Polymerization of Allene and 1,3-Dienes

Giovanni Ricci [1,*], Antonella Caterina Boccia [1], Giuseppe Leone [1] and Alessandra Forni [2]

[1] CNR, Istituto per lo Studio delle Macromolecole (ISMAC), via A. Corti 12, I-20133 Milano, Italy; antonella.boccia@ismac.cnr.it (A.C.B.); giuseppe.leone@ismac.cnr.it (G.L.)

[2] CNR, Istituto di Scienze e Tecnologie Molecolari (ISTM), Università degli Studi di Milano, via C. Golgi 19, I-20133 Milano, Italy; alessandra.forni@istm.cnr.it

* Correspondence: giovanni.ricci@ismac.cnr.it; Tel.: +39-02-2369-9376

Received: 16 November 2017; Accepted: 1 December 2017; Published: 7 December 2017

Abstract: Novel allyl cobalt complexes, i.e., (η^3-C_4H_7)(η^4-C_4H_6)Co($PCyPh_2$) (**1**), (η^3-C_4H_7)(η^4-C_4H_6)Co($PMePh_2$) (**2**) and (η^3-C_5H_9)(η^4-C_5H_8)Co($PMePh_2$) (**3**), were synthesized by reacting $CoCl_2(PRPh_2)_2$ (R = methyl, cyclohexyl) with 1,3-butadiene or isoprene in presence of metallic zinc. The complexes were fully characterized by Nuclear Magnetic Resonance (NMR) spectroscopy (^{1}H and 2D experiments); in case of **1**, single crystals, suitable for X-ray analysis, were obtained and the molecular structure was determined. The allyl cobalt phosphine complexes alone gave highly crystalline 1,2 polymers from 1,2-propadiene, but they did not polymerize 1,3-dienes. Nevertheless, in the presence of a stoichiometric amount of methylaluminoxane (MAO), they were able to polymerize 1,3-butadiene and substituted 1,3-butadienes such as isoprene, (*E*)-1,3-pentadiene, (*E*)-1,3-hexadiene, and (*E*)-3-methyl-1,3-pentadiene. Specifically, **1**/MAO gave predominantly syndiotactic 1,2 polymers from 1,3-butadiene and terminally substituted 1,3-butadienes (e.g., 1,3-pentadiene and 1,3-hexadiene), but it was practically not active in the polymerization of internally substituted 1,3-butadienes (e.g., isoprene and 3-methyl-1,3-pentadiene); **2**/MAO and **3**/MAO exhibited instead an opposite behavior, giving predominantly isotactic 1,2 polymers from 3-methyl-1,3-pentadiene, and showing very low activity in the polymerization of 1,3-butadiene, 1,3-pentadiene and 1,3-hexadiene. The results obtained are interesting from the mechanistic point of view, and some hypotheses to explain this particular behavior were formulated.

Keywords: allyl cobalt phosphine complexes; X-ray structure; NMR characterization; 1,3-butadiene; polymerization of conjugated dienes; 1,2-polyallene

1. Introduction

Transition metal catalysts commonly used for the polymerization of 1,3-dienes can be grouped into the following classes: (i) catalysts derived from aluminum compounds (i.e., aluminum alkyls, aluminum hydrides and aluminoxanes) and transition metal compounds (Ziegler–Natta catalysts); (ii) catalysts derived from precursors not containing preformed metal-carbon bonds; (iii) catalysts based on allyl derivatives of transition metals [1–5]. Ziegler–Natta catalysts are obviously the most important ones, they can be highly active and stereospecific, and are industrially used for the production of *cis*-1,4 poly(1,3-butadiene), *cis*-1,4 polyisoprene and 1,2 syndiotactic poly(1,3-butadiene), the only diene polymers of industrial interest.

Extensive work has also been carried out with catalysts based on transition metal allyl derivatives [1]; these systems, which include simple allyl derivatives of transition metals and more

complex catalysts derived from the reaction of the allyl complexes with electron donors, electron acceptors or Lewis acids, are of particular interest mainly because they are good models of the active site structure, and therefore provide useful information to elucidate the catalysis of polymerization.

The first examples of stereospecific polymerization induced by simple allyl derivatives of transition metals were first reported in 1964. A predominantly 1,2 poly(1,3-butadiene) was obtained with $(allyl)_3Cr$ and a predominantly *cis*-1,4 polymer with $(allyl)_2CoI$ [6]. A crystalline poly(1,3-butadiene) consisting almost exclusively of *trans*-1,4 units and a predominantly *cis*-1,4 polymer were obtained with (allyl)NiBr depending on the type of polymerization solvent used [7]. Allyl derivatives of other transition metals (Ti, Zr, Mo, W, Ru, Rh, U, Nd) were later found to be effective catalysts [8–10]. More recently, the allyl cobalt compound $(\eta^4\text{-}C_4H_6)(\eta^5\text{-}C_8H_{13})Co$, alone or in presence of CS_2, was reported to be highly active and stereoselective in the polymerization of 1,3-butadiene to 1,2 syndiotactic polymer [11–15].

We have now synthesized three novel allyl cobalt compounds $(\eta^3\text{-}C_4H_7)(\eta^4\text{-}C_4H_6)Co(PCyPh_2)$ (**1**), $(\eta^3\text{-}C_4H_7)(\eta^4\text{-}C_4H_6)Co(PMePh_2)$ (**2**) and $(\eta^3\text{-}C_5H_9)(\eta^4\text{-}C_5H_8)Co(PMePh_2)$ (**3**). The complexes were characterized by Nuclear Magnetic Resonanance (NMR) (^1H and 2D experiments) and X-ray diffraction analysis, and their behavior in the polymerization of 1,2-propadiene and various 1,3-dienes was investigated. The most significant results obtained are reported in this paper.

2. Results

2.1. Synthesis and Characterization of the Cobalt Phosphine Complexes

The allyl cobalt phosphine **1**–**3** complexes were prepared by reacting $CoCl_2(PRPh_2)_2$ (R = methyl, cyclohexyl) with 1,3-butadiene or isoprene in presence of metallic zinc (Scheme 1), according to the experimental procedure already described in the literature for analogous complexes [16,17].

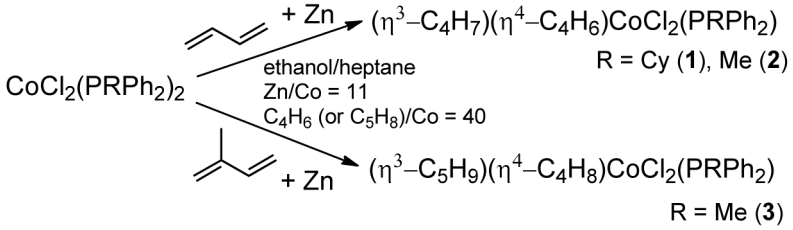

Scheme 1. Synthesis of the allyl cobalt phosphine complexes.

2.1.1. X-ray Crystal Structure and Computational Analysis

In case of $(\eta^3\text{-}C_4H_7)(\eta^4\text{-}C_4H_6)Co(PCyPh_2)$ (**1**), single crystals suitable for X-ray structure determination were obtained. The molecular structure is shown in Figure 1, while selected bond lengths and angles, and crystallographic data are reported in Tables 1 and S1, respectively. Structural analysis reveals that the coordination sphere around the cobalt ion comprises, besides the phosphine ligand, the C1–C3 allyl group and the C5–C8 butadiene molecule, with the C1, C2 allylic carbons and the C6, C7 central atoms of butadiene closest to Co with respect to C3 and the butadiene lateral carbons C5 and C8, respectively.

The allylic unit and the butadiene molecule face approximately parallel to each other, the dihedral angle between their respective least-squares planes measuring 13(1)°. Within the phosphine unit, the P–C bond lengths are slightly shorter for the aromatic with respect to the aliphatic carbon atoms, as expected. Comparison with the only structurally related cobalt complex reported in literature, i.e., $(\eta^3\text{-}C_4H_7)(\eta^4\text{-}C_4H_6)Co(PPh_3)$ [16], shows that the most evident differences with the present structure are found in the torsion angle C1–C2–C3–C4, θ, which is 47(2)° in the former and −173.9(7)° in the latter, and in the spatial disposition of the phosphinic ligand with respect to the allyl/butadiene moieties. Such conformational differences appear to be correlated. In fact, considering the plane containing the

Co–P bond and roughly parallel to the C1–C3 and C5–C8 least-squares planes (which are not strictly parallel as noted above), one phenyl ring of the structure with PPh_3 [16] lies approximately in this plane, i.e., midway between the allylic unit and the butadiene molecule, and points on the same side as the C4 methyl group.

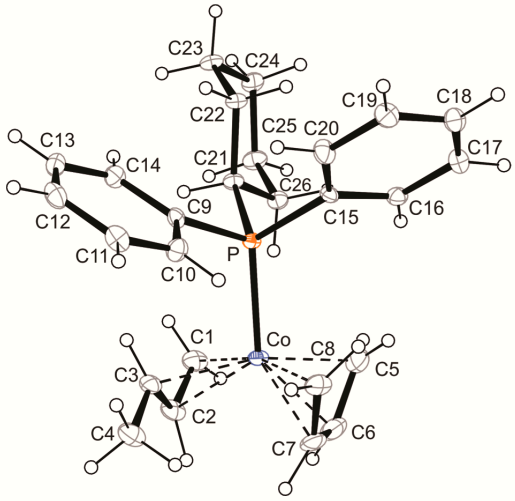

Figure 1. Molecular structure of (η^3-C_4H_7)(η^4-C_4H_6)Co($PCyPh_2$) (**1**) with thermal ellipsoids drawn at 30% probability level.

The consequent Ph/Me repulsion is alleviated by a moderate deviation of the methyl from the perfect, more stable, *anti* geometry ($\theta = 0°$). In the present structure, on the other hand, the $PCyPh_2$ ligand is rotated around the Co–P bond in such a way as to bring the bulkier Cy ring as far away from the methyl group. The large Ph/Me repulsion which would arise in such a conformation is avoided by a further rotation of the methyl towards the less stable *syn* geometry ($\theta = 180°$).

Table 1. Selected X-ray Bond Lengths (Å) and Angles (°) for complex **1**.

Co–P	2.2049(16)	C1–C2	1.406(10)	C1–Co–P	99.3(2)
		C2–C3	1.405(10)	C2–Co–P	120.3(2)
Co–C1	2.066(7)	C3–C4	1.503(10)	C3–Co–P	96.8(2)
Co–C2	1.996(7)	C5–C6	1.405(12)	C5–Co–P	99.5(2)
Co–C3	2.123(7)	C6–C7	1.420(12)	C6–Co–P	137.7(3)
Co–C4	3.192(8)	C7–C8	1.397(10)	C7–Co–P	134.3(2)
Co–C5	2.083(8)			C8–Co–P	95.3(2)
Co–C6	2.010(7)	P–C9	1.841(6)		
Co–C7	2.006(7)	P–C15	1.839(6)		
Co–C8	2.085(7)	P–C21	1.854(6)		

Subtler but not negligible differences are found in bond lengths. The Co–P bond is elongated by 0.014 Å (from 2.191(4) [16] to 2.2049(16) Å) as a result of the replacement of one aromatic phenyl unit with the aliphatic cyclohexyl ring, which decreases the π–character of the Co–P bond and increases the steric hindrance of the phosphine ligand. On the side of the π–system coordination, on the contrary, the Co–C bond lengths are systematically shorter in the present structure, suggesting a greater π–character for these bonds. Although such differences in bond lengths are at the limit of the experimental accuracy, they are partially reproduced by Density Functional Theory (DFT) calculations in gas phase (Table 2). They provide a Co–P lengthening, equal to 0.021 Å, and a slight shortening in the Co–C(allyl) bond lengths going from PPh_3 to $PCyPh_2$. The butadiene molecule is instead approximately at the same distance from the Co ion. Interestingly, the simulated structure of (η^3-C_4H_7)(η^4-C_4H_6)Co($PMePh_2$) (**2**) features the shorter Co–P and Co–C(allyl) bonds within the series

of the three complexes. The $PMePh_2$ phosphine ligand shares in fact the same π–character as $PCyPh_2$, but its sterical hindrance is drastically lower, allowing a significant approaching to the cobalt ion.

Table 2. Selected M06/6-311g(d) computed bond lengths (Å) for $(\eta^3\text{-}C_4H_7)(\eta^4\text{-}C_4H_6)Co(PRPh_2)$ with R = cyclohexyl (Cy), phenyl (Ph) and methyl (Me).

Bond	$PCyPh_2$	PPh_3	$PMePh_2$
Co–P	2.233	2.212	2.206
Co–C1	2.044	2.050	2.039
Co–C2	1.995	1.999	1.990
Co–C3	2.089	2.093	2.084
Co–C5	2.053	2.053	2.045
Co–C6	1.999	2.001	1.999
Co–C7	2.006	2.003	2.006
Co–C8	2.058	2.049	2.056
C1–C2	1.412	1.409	1.413
C2–C3	1.403	1.403	1.406
C3–C4	1.495	1.496	1.496
C5–C6	1.410	1.411	1.411
C6–C7	1.415	1.415	1.415
C7–C8	1.411	1.413	1.411

In the crystal structure of complex **1**, several H–H intramolecular distances are found below or slightly above two times the H atom van der Waals radius, involving the butadiene and the allyl group (H2–H6, 2.41 Å; H4C–H7, 2.23 Å); the butadiene and either phenyl groups (H5A–H20, 2.25 Å; H8A–H10, 2.41 Å), or the Cy ring (H5B–H26B, 2.49 Å); the allylic group and the Cy ring (H1B–H21, 2.50 Å and H1B–H26B, 2.52 Å); the Ph and the Cy phosphinic units (H14–H21, 2.18 Å, H14–H22A, 2.16 Å and H20–H26A, 2.33 Å).

2.1.2. NMR Characterization

The ^1H NMR spectra of $(\eta^3\text{-}C_4H_7)(\eta^4\text{-}C_4H_6)Co(PCyPh_2)$ (**1**) and $(\eta^3\text{-}C_4H_7)(\eta^4\text{-}C_4H_6)Co(PMePh_2)$ (**2**) are shown in Figure 2a,b, respectively. Protons of the allyl unit and of the coordinated butadiene monomer were assigned referring to the integrals, multiplicity, and chemical shifts in the ^1H NMR spectra, and to the ^1H–^1H correlations in TOtal Correlation SpectroscopY (TOCSY) experiments (Figures 3 and S1). Information concerning the spatial reciprocal orientation of the allylic unit and of the butadiene monomer coordinated to the cobalt atom can be deduced from the ^1H–^1H correlations in Rotating frame Overhauser Effect SpectroscopY (ROESY) experiments (see below in the text).

The ^1H spectrum of **1** (Figure 2a) was assigned as follows: H_i and H_e, multiplet, as sum of two triplets, at $\delta = -0.24$ ppm; H_d, triplet at $\delta = 0.30$ ppm, J_{db} 11 Hz; Me, doublet at $\delta = 0.87$ ppm; H_c, merging signal at $\delta = 1.02$ ppm; H_k and H_f, two doublets at $\delta = 1.60$ and $\delta = 2.22$ ppm; H_a, broad doublet at $\delta = 1.77$ ppm; H_b, multiplet at $\delta = 4.26$ ppm; H_g and $H_{g'}$, two multiplets at $\delta = 4.36$ and 4.45 ppm respectively, J_{gk} 7 Hz, J_{ge} 12 Hz; H_{cy}, signals at $\delta = 0.80$, 0.99, 1.21, 1.59, 2.22, and 2.42 ppm; H_{ar}, doublet at $\delta = 7.13$ ppm, and two overlapping triplets at $\delta = 7.62$ and 7.68 ppm, respectively. The up-field shift for the anti (H_e and H_i) protons of butadiene, Figure 2a, seems to suggest a partial σ character of the bond between the cobalt atom and C1, C4 carbon atoms of coordinated butadiene, in agreement with those previously reported [17]. Protons H_g and $H_{g'}$ are low field shifted as expected for the olefin carbons C2 and C3 of the butadiene unit. To distinguish the $H_g/H_{g'}$ protons from H_b and to confirm the above reported assignment the ^1H–^1H TOCSY experiments (Figure 3) were of a great help. Because only $H_{i,e}$ and $H_{g,g'}$ are relative to the same spin system, it is expected that they generate two partially merging cross peaks on the TOCSY spectrum (namely 1 and 2 in Figure 3). Moreover, the protons of the cyclohexyl group of the phosphine ligand were unambiguously solved also if present in a very crowded region in the ^1H spectrum.

The ^1H NMR spectrum of complex **2** (Figure 2b) was assigned as follows, by applying the same strategy reported above for the other cobalt complex: $H_{i,e}$ protons, two triplets at $\delta = -1.21$ ppm

and −0.51 ppm, $J_{i,e/g,g'}$ 11 Hz; methyl protons of the allylic unit, two superimposed doublets at δ = 0.37 ppm, $J_{Me/a,b}$ 7 Hz; H_d, triplet at δ = 0.93 ppm; methyl protons of the methyl group bonded to the phosphorus atom, doublet at δ = 1.96 ppm, $J_{Me,d}$ 6.7 Hz; $H_{k,f}$, two doublets at δ = 2.08 and 2.40 ppm, $J_{k,f/g,g'}$ 7 Hz; H_c, merging signal with $H_{k,f}$ at δ = 2.08 ppm; H_a, multiplet at δ = 2.79 ppm; $H_{g,g'}$, two multiplets at δ = 4.23 and 4.47 ppm; H_b, multiplet at δ = 4.58 ppm; aryl protons H_{ar} of the phosphine ligand at δ = 7.09, 7.55, and 7.68 ppm. Uncertainties about some closer resonances were solved by TOCSY experiments (Figure S1). In fact, H_g and $H_{g'}$ were distinguished from H_b as they are part of the same spin system and they have to correlate with each other.

complex\ppm	H_a	H_b	H_c	H_d	H_e/H_i	H_f/H_k	$H_g/H_{g'}$	Me
1 *syn* (η^3-C_4H_7)(η^4-C_4H_6)Co($PCyPh_2$)	1.77	4.26	1.02	0.30	-0.24	1.60 2.22	4.36 4.45	0.87
2 *anti* (η^3-C_4H_7)(η^4-C_4H_6)Co($PMePh_2$)	2.79	4.58	2.08	0.93	-1.21 -0.51	2.08 2.40	4.23 4.47	0.37

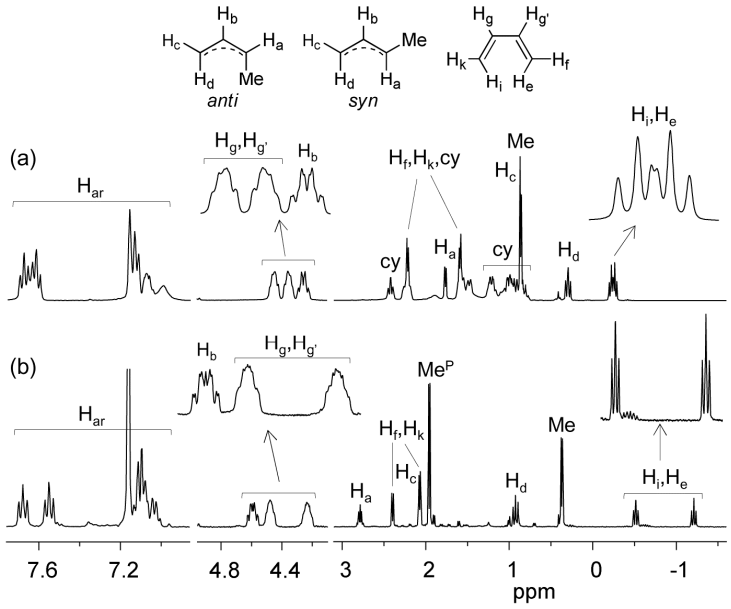

Figure 2. ^{1}H NMR spectra of (**a**) (η^3-C_4H_7)(η^4-C_4H_6)Co($PCyPh_2$) (**1**) and (**b**) (η^3-C_4H_7)(η^4-C_4H_6)Co($PMePh_2$) (**2**) (Me^P indicates the protons of the methyl on the ligand phosphorus atom, H_{ar} = aryl protons, cy = cyclohexyl protons).

The ^{1}H NMR spectrum of (η^3-C_5H_9)(η^4-C_5H_8)Co($PMePh_2$) (**3**) is shown in Figure 4, and it was assigned as follows. ^{1}H spectrum: H_e, doublet at δ = −1.40 ppm, $J_{e/f}$ 13 Hz; H_i, triplet at δ = −0.56 ppm, $J_{i/g}$ 11 Hz; H_{Me}, singlet at δ = 0.38 ppm; H_d, triplet at δ = 0.67 ppm, $J_{d/b}$ 12 Hz; H_{Me}, singlet at δ = and 1.21 ppm; H_c, doublet at δ = 1.55 ppm, $J_{c/b}$ 7 Hz; $H_{Me''}$, doublet at δ = 1.62 ppm; H_f, singlet at δ = 1.78 ppm; H_k, doublet at δ = 1.93 ppm; $H_{Me/P}$, signal partially merging with H_k at δ = 1.93 ppm; H_b, broad triplet at δ = 4.20 ppm; H_g, triplet at δ = 4.35 ppm, $J_{g/k}$ 8 Hz; H_{ar}, signals at δ = 7.13, 7.50 and 7.68 ppm. ^{1}H–^{1}H TOCSY experiment confirms the exact assignment of protons spin system (Figure S2).

On the basis of the above, it appears evident that the most significant ^{1}H NMR signals permitting to discriminate between the three different complexes are those related to the following protons: allyl methyl (Me), $H_{i/e}$, $H_{g/g'}$ and H_b. The ppm values of the allyl methyl protons are clearly indicative of the type of allyl unit configuration (*anti* or *syn*) [17], while the ppm values and multiplicities of $H_{i/e}$, $H_{g/g'}$ and H_b are most likely related to the type of reciprocal monomer/allyl unit orientation (*exo-exo* or *exo-endo*). Further work is certainly needed (e.g., synthesis of allyl cobalt complexes with different phosphine ligands; further NMR experiments, also at variable temperature) in order to confirm these indications.

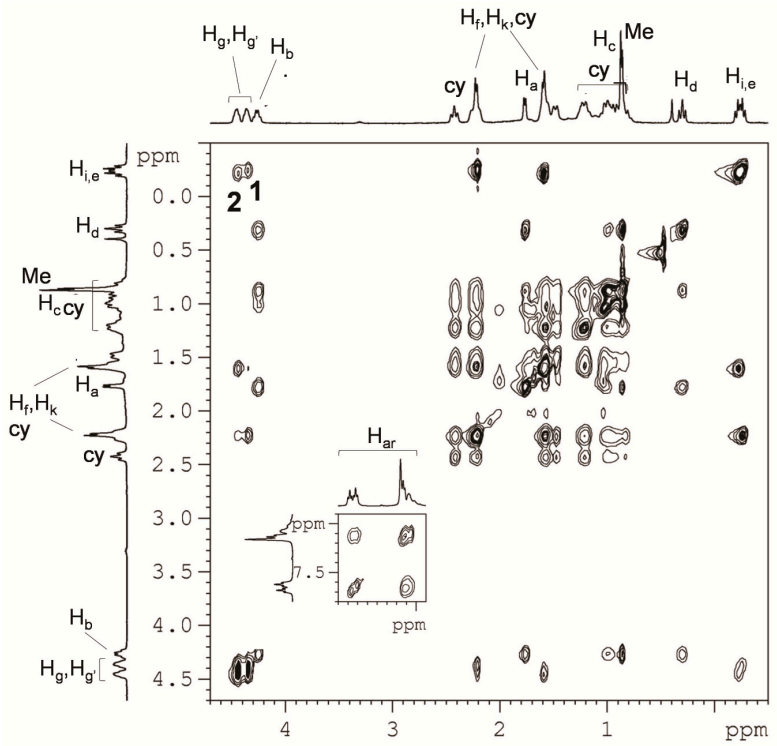

Figure 3. TOCSY NMR spectrum of (η^3-C_4H_7)(η^4-C_4H_6)Co(PCyPh$_2$) (**1**).

complex\ppm	H_a	H_b	H_c	H_d	H_e	H_i	H_f	H_g	H_k	Me	Me'	Me''	Me^P
3 *syn* (η^3-C_5H_9)(η^4-C_5H_8) Co(PMePh$_2$)	-	4.20	1.55	0.67	-1.40	-0.56	1.78	4.35	1.93	0.38	1.21	1.62	1.93

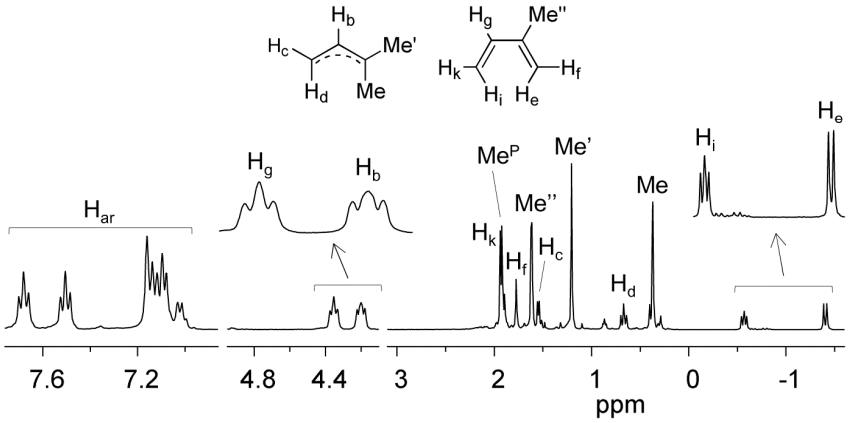

Figure 4. ^{1}H NMR spectra of (η^3-C_5H_9)(η^4-C_5H_8)Co(PMePh$_2$) (**3**) (Me^P indicates the protons of the methyl on the ligand phosphorus atom, H_{ar} = aryl protons).

In order to get information about the reciprocal spatial rearrangement of the allylic unit and of the butadiene (or isoprene) monomer in the three different cobalt complexes synthesized, ^{1}H–^{1}H ROESY experiments were acquired (Figures 5, S3 and S4). In case of ^{1}H–^{1}H ROESY experiment of complex **1** (Figure 5), correlations of the aromatic aryl protons on the phosphorus atom, at δ = 7.68 ppm, with some aliphatic protons, put in evidence the spatial vicinity between the phosphine ligand and the allylic and butadiene units, thus providing information on the reciprocal orientation of these two units. As can be observed in Figure 5, aryl protons of the phosphine ligand at 7.68 ppm correlate with (i) the

cyclohexyl protons of the same phosphine ligand; (ii) the protons H_i and H_e of the butadiene monomer (*cross-peak 1*); (iii) the H_d and H_a protons of the allylic unit (*cross-peaks 2* and *3*, respectively). Moreover, the cyclohexyl proton at δ = 2.42 ppm correlates with the $H_{i,e}$ and H_d protons (*cross-peaks 4* and *5*) of the allylic and butadiene unit, respectively, while no correlations are observed with the protons $H_{g,g'}$ and H_b, thus in agreement with the reciprocal *exo-exo* spatial orientation of the allylic unit and the butadiene monomer shown by the X-ray molecular structure of complex **1** (Figure 1). Finally, a *syn* configuration for the allyl unit was suggested by the strong correlation between H_a and H_d protons, again in agreement with the crystalline structure of **1**.

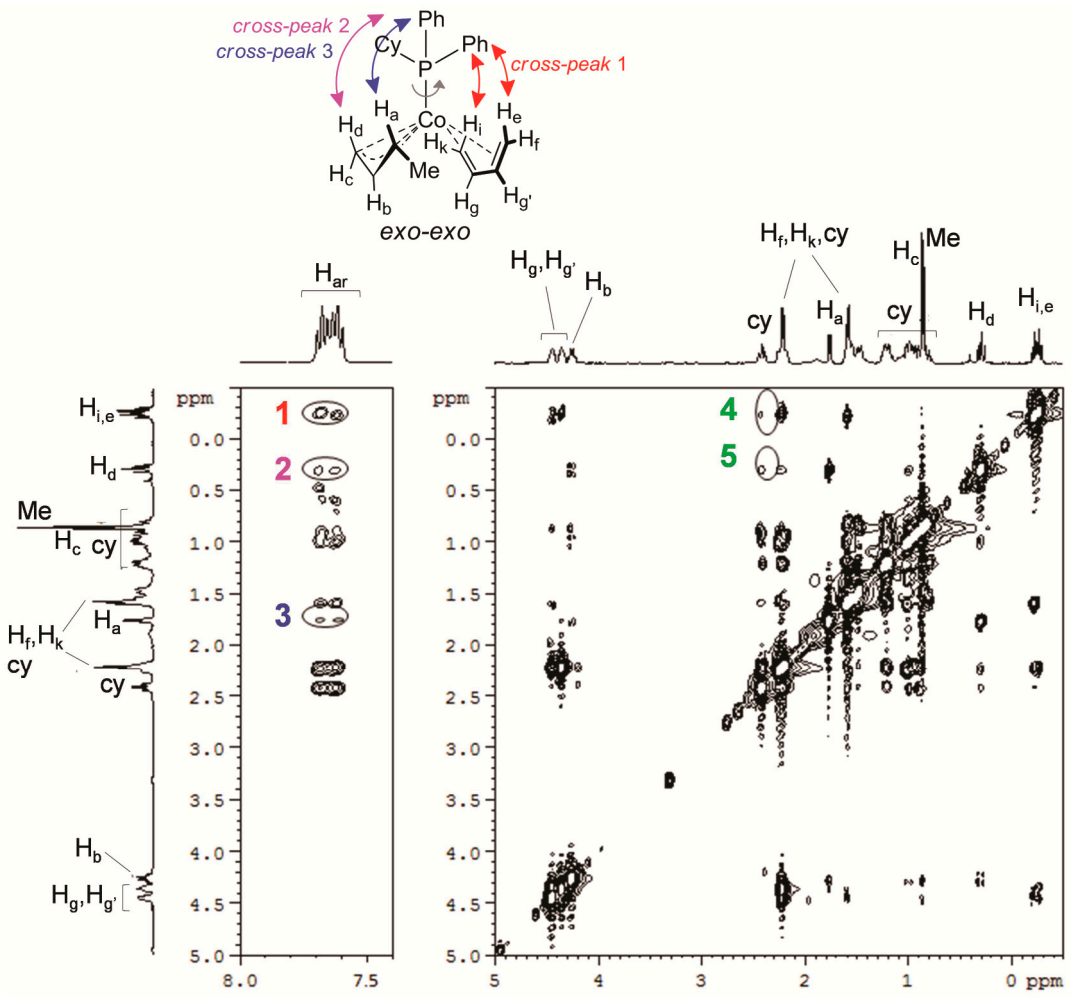

Figure 5. ROESY NMR spectrum of $(\eta^3\text{-}C_4H_7)(\eta^4\text{-}C_4H_6)Co(PCyPh_2)$ (**1**).

As concern the reciprocal spatial orientation of the isoprene monomer and of allylic unit in case of $(\eta^3\text{-}C_5H_9)(\eta^4\text{-}C_5H_8)Co(PMePh_2)$ (**3**), the ROESY experiments (Figure S3) seem instead to suggest the presence of an *exo-endo* orientation, or anyway the coexistence of both the orientations, *exo-endo* (Figure 6A) and *exo-exo* (Figure 6B). The methyl-*anti* (Me) at 0.38 ppm and methyl-*syn* (Me') protons at 1.21 ppm of the allylic unit spatially correlate with the H-aryl's on the phosphine (*cross peaks 1* and *2*, the *cross-peak 2* being less intense because "*less close*" to the corresponding Me' group (Figure S3)). In addition, as only Me protons at δ = 0.38 ppm correlate with Me on the phosphine (Me^P at 1.93 ppm), it is possible to affirm that Me-*anti* is oriented on the same side of the phosphine ligands, confirming indeed the *syn/anti* attribution of the two methyl groups Me and Me' and the *exo* orientation of the allylic unit. Moreover, the H_g and $H_{Me'}$ interaction (*cross peak 3*, Figure S3) seems to suggest that they are oriented on the same side, that is compatible with an *exo-endo* reciprocal orientation of the allylic

group and of the isoprene unit (Figure 6A); on the other hand the complete absence of any interactions between $H_{i,e}$ and $H_{f,k}$ with the aryl and methyl protons of the phosphine ligand are also in favor of an *exo-endo* orientation of the allylic group and of the isoprene unit. This means that when the phosphine ligand is $PMePh_2$, both the arrangements (*exo-exo* and *exo-endo*) are possible, in agreement indeed with the formation of atactic 1,2 polymers in the polymerization of terminally substituted monomers such as 1,3-pentadiene and 1,3-hexadiene [18] with catalyst based on complex **3**, as reported below in the text.

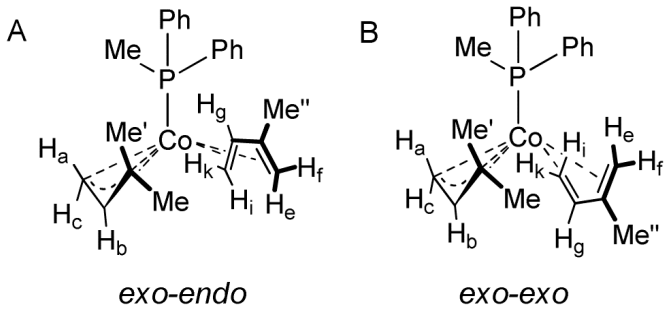

Figure 6. Possible reciprocal spatial orientations of the allyl group and the isoprene monomer for $(\eta^3\text{-}C_5H_9)(\eta^4\text{-}C_5H_8)Co(PMePh_2)$ (**3**): *exo-endo* (**A**) and *exo-exo* (**B**).

The ROESY experiments carried out on complex **2** (Figure S4) seem to suggest a situation very close to that found for complex **3**. No correlations involving allylic protons (H_a, H_b, H_c) and the protons of the aryl phosphine ligand were detected, while some experiments reveal a weak correlation between the methyl group (*syn*) of the allylic unit and the aryl protons, that is what expected for an *exo* rearrangement of the allylic group. As regard the orientation of the 1,3-butadiene monomer, in all the ROESY experiments carried out, only one proton of the butadiene monomer, H_f or H_k, at δ = 2.40 ppm, (*cross-peak 1*, Figure S4), was found to spatially correlate with protons of the aryl phosphine ligand, at δ = 7.68 and 7.55 ppm, suggesting indeed an *exo* orientation of butadiene; however, the H_g proton was found to correlate with the methyl protons of the allylic group, in agreement in this case with an *endo* orientation of the butadiene monomer. It follows indeed that, as occurred in the case of complex **3**, both orientations, *exo-exo* and *exo-endo*, are possible, indicating some fluxionality of the butadiene monomer coordinated to the cobalt atom.

2.2. Polymerization

2.2.1. Polymerization of 1,2 Propadiene

The allyl cobalt complexes alone do not polymerize 1,3-dienes, as we will see later, while they show a rather low activity in the polymerization of 1,2-propadiene (Table 3), giving highly stereoregular crystalline 1,2 polymers with a melting point of about 110 °C (Figure 7a,b). As an example, the ^{13}C NMR spectrum of the poly(1,2-propadiene) obtained with $(\eta^3\text{-}C_4H_7)(\eta^4\text{-}C_4H_6)Co(PMePh_2)$ (Table 3, run 2) is shown in Figure 7c. It is worth noting that complex **3** was more active than **1** and **2**, likely due to its lower stability and/or greater reactivity toward the interaction with MAO.

Table 3. Polymerization of 1,2-propadiene with cobalt complexes **1**–**3** [a].

Entry	Catalyst	Time (h)	Yield (g)	M_w ($\times 10^3$)	M_w/M_n
1	1/MAO	2	0.05	22	3.2
2	2/MAO	1.5	0.17	21	3.8
3	2	21	0.14	18	2.8
4	3/MAO	1	0.59	35	2.9

[a] Polymerization conditions: 1,2 propadiene, 2 mL; toluene, total volume 16 mL; MAO/Co = 2; Co, 5×10^{-5} mol; temperature, 22 °C.

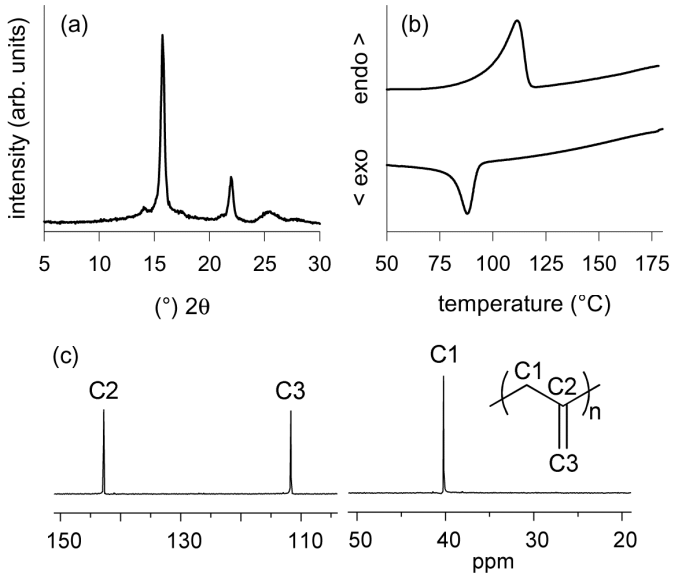

Figure 7. Powder X-ray Diffraction (PXRD) (**a**); Differential Scanning Calorimetry (DSC) (**b**) and ^{13}C NMR (**c**) spectra of poly(1,2-propadiene) (Table 3, entry 2).

2.2.2. Polymerization of 1,3 Dienes

As mentioned above, the allyl cobalt complexes alone do not polymerize 1,3-dienes. They become, however, active in the presence of small amounts (stoichiometric) of MAO, as shown in Table 4. Predominantly 1,2 polymers were obtained from 1,3-butadiene; (η^3-C_4H_7)(η^4-C_4H_6)Co($PCyPh_2$) (**1**) exhibited a quite good activity, giving predominantly syndiotactic polymers, while (η^3-C_4H_7)(η^4-C_4H_6)Co($PMePh_2$) (**2**) and (η^3-C_5H_9)(η^4-C_5H_8)Co($PMePh_2$) (**3**) were characterized by a rather low activity and stereospecificity, giving essentially atactic 1,2 polymers.

The allyl cobalt complexes were also able to polymerize substituted 1,3-butadienes such as (*E*)-1,3-pentadiene, (*E*)-1,3-hexadiene, isoprene and (*E*)-3-methyl-1,3-pentadiene. Complex **1** resulted to be highly active and selective in the polymerization of 1,3-pentadiene and 1,3-hexadiene, giving crystalline, highly syndiotactic 1,2 polymers, while it was almost inactive in the polymerization of isoprene and 3-methyl-1,3-pentadiene.

On the contrary, complexes **2** and **3** were highly active in the polymerization of isoprene and 3-methyl-1,3-pentadiene, while only polymer traces were obtained from 1,3-pentadiene and 1,3-hexadiene. Furthermore, they gave a predominantly isotactic polymer from 3-methyl-1,3-pentadiene and an alternate *cis*-1,4-*alt*-3,4 polymer from isoprene [19].

Table 4. Polymerization of 1,3-dienes with cobalt complexes **1**–**3** [a].

Entry	Catalyst	Time (h)	Yield (g)	Conv. (%)	1,2 [b] (mol%)	rr/mr/mm [c]	M_w ($\times 10^3$)	M_w/M_n
1,3-butadiene								
1	1	168	-					
2	2	168	-					
3	3	168	-					
4	1/MAO	2	0.87	62	87	71/25/4	169	2.4
5	2/MAO	15	0.20	14	73	26/48/26	160	2.5
6	3/MAO	10	traces					
E-1,3-pentadiene								
7	1/MAO	15	1.24	91	≥99	69/31/0	150	1.7
8	2/MAO	24	0.26	19	≥99	24/50/26	97	1.6
1,3-hexadiene								
9	1/MAO	12	0.66	46	≥99	72/28/0	74	1.9
10	2/MAO	144	0.18	13	≥99	22/51/27	55	1.6
isoprene								
11	1/MAO	24	traces					
12	2/MAO	24	0.45	33	~50		68	1.5
13	3/MAO	24	0.51	38	~50		75	1.4
3-methyl-1,3-pentadiene								
14	1/MAO	24	traces					
15	2/MAO	24	0.94	64	100	0/0/100	90	1.2
16	3//MAO	24	0.85	58	100	0/0/100	87	1.3

[a] Polymerization conditions: monomer, 2 mL; toluene as solvent, total volume 16 mL; MAO/Co molar ratio 2–3; Co, 5×10^{-5} mol; temperature, 22 °C. [b] mol% of 1,2 units (3,4 in case of isoprene), the remaining units are essentially *cis*-1,4. [c] percentage of syndiotactic/atactic/isotactic triads, determined by ^{13}C NMR.

3. Discussion

The reasons why (i) the above allyl complexes become active only when used in combination with MAO and (ii) some complexes (e.g., **1**) are highly active and selective in the polymerization of 1,3-butadiene, 1,3-pentadiene and 1,3 hexadiene (i.e., terminally substituted 1,3-butadienes) and not in case of isoprene and 3-methyl-1,3-pentadiene (i.e., internal substituted 1,3-butadienes), while other complexes (e.g., **2** and **3**) exhibit a completely opposite behavior being highly active and selective in the polymerization of isoprene and 3-methyl-1,3-pentadiene (i.e., internal substituted 1,3-butadienes) and not in case of 1,3-butadiene, 1,3-pentadiene and 1,3-hexadiene, are somewhat difficult to explain and to rationalize.

A tentative interpretation for the role of MAO is shown in Scheme 2. In principle, MAO can interact with the metal complex in three different ways (Scheme 2): by extracting the allyl group as in route a; by extracting the phosphine ligand as in route b; by coordinating through the oxygen atom to the cobalt atom, thus destabilizing in some way the cobalt complex, and favoring the insertion of the diene monomer at C3 of the allyl group, as shown in route c. According to route a, no metal-carbon bond for the monomer insertion is available; following route b no more ligand remains coordinated to the cobalt atom, meaning that we should not observe any influence of the ligand on the polymerization stereoselectivity, while, as reported above, 1,2 poly(1,3-butadiene)s having different tacticity, depending on the type of ligand coordinated to the cobalt atom, are obtained. It follows indeed that route c appears to be the most probable one. This hypothesis, in our opinion, is also in agreement with the fact that allene can be polymerized also in absence of MAO; allene could coordinate with only one double bond, thus favoring the insertion of the coordinated 1,3-butadiene, and then inserting itself into the allyl group of the growing chain. On the other hand, a similar behavior was observed with the allyl cobalt complex (η^4-C_4H_6)(η^5-C_8H_{13})Co, which was found to be extremely active in the polymerization of 1,3-butadiene to 1,2 polymers only if used in combination with CS_2 [12,15].

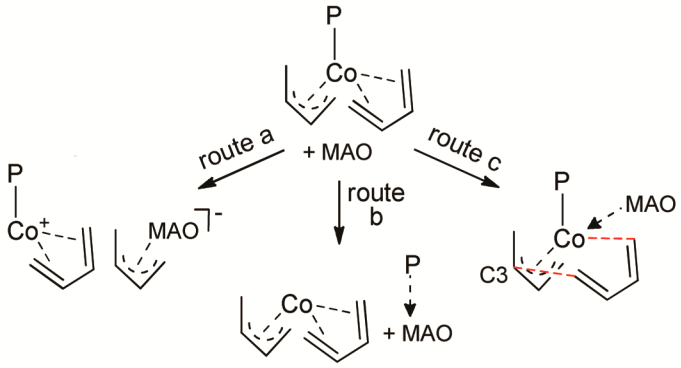

Scheme 2. Simplified illustration of the possible interactions between MAO and the allyl cobalt complexes.

The different behavior, regarding activity and stereospecificity, exhibited by the various cobalt complexes in the polymerization of the different diene monomers is even more difficult to interpret, but it is, in some way, in agreement with that observed in the polymerization of 1,3-dienes with the catalytic systems $CoCl_2(PRPh_2)_2$/MAO (R = methyl, ethyl *n*-propyl, *i*-propyl, cyclohexyl) [20,21]. We reported in previous papers that, in general, the stereoselectivity in the polymerization of 1,3-dienes with transition metal complex-based catalysts [e.g., $CrCl_2(L)$/MAO (L = bidentate phosphine); $FeCl_2(L)_2$-MAO (L = phenanthroline); $CoCl_2(L)_2$/MAO (L = monodentate phosphine)] was strongly affected by the catalyst structure (i.e., type of ligand bonded to the metal atom) and by the monomer structure [22–30]. The obtained results clearly indicated that (i) the *exo-exo* orientation of the allyl group of the growing chain and of the coordinated monomer was strongly favored in case of 1,3-butadiene and terminally substituted monomers, and of hindered ligands on the cobalt atom; (ii) the *exo-endo* orientation was instead favored in case of internally substituted 1,3-butadienes (e.g., isoprene and 3-methyl-1,3-pentadiene) and low hindered ligands on the metal atom [18]. Such a behavior is now confirmed, and even more evident, in case of the polymerization of 1,3-dienes with the allyl cobalt complexes object of the present paper. Complex **1**, exhibiting an *exo-exo* orientation of allyl group/coordinated monomer, is very active and selective only with terminally substituted monomers, that is monomers preferring such an orientation, while it is almost inactive with internally substituted monomers (isoprene and 3-methyl-1,3-pentadiene), that is monomers having higher affinity for the *exo-endo* orientation. The cobalt complexs **2** and **3**, for which the NMR analysis indicated the presence of both the orientations, *exo-endo* (probably the preferred one) and *exo-exo*, resulted instead scarcely active and selective with terminally substituted 1,3-butadienes, that is monomers preferring *exo-exo* orientations (e.g., 1,3-butadiene, 1,3-pentadiene and 1,3-hexadiene), while they were extremely active and selective in the polymerization of isoprene and 3-methyl-1,3-pentadiene, monomers preferring *exo-endo* orientations. Obviously, what is reported above has to be considered only a working hypothesis to provide a plausible interpretation for the obtained results and to stimulate discussion on this topic; further experimentation will be necessary and will be carried out to confirm or deny such an interpretation.

4. Materials and Methods

4.1. Materials

Anhydrous cobalt dichloride (Aldrich, St. Louis, MO USA, 99.9% pure), Zn powder (Strem, Newburyport, MA, USA, 99.9%), and methylaluminoxane (MAO) (Aldrich, 10 wt % solution in toluene) were used as received. Ethyl alcohol (Aldrich, 96%) was degassed under vacuum, then by bubbling dry dinitrogen and kept over molecular sieves; heptane (Aldrich, >99%) was refluxed over Na/K alloy for 8 h, then distilled and stored over molecular sieves under dry dinitrogen; toluene

(Aldrich, 99.5%) was refluxed over Na for 8 h, then distilled and stored over molecular sieves under dry nitrogen. 1,2 propadiene (Aldrich, ≥96%) was used as received. 1,3-Butadiene (Air Liquide, Paris, France, >99.5%) was evaporated from the container prior to each run, dried by passing through a column packed with molecular sieves and condensed into the reactor which had been precooled to −20 °C. Isoprene (Aldrich ≥99.5%), (*E*)-1,3-pentadiene (Aldrich, ≥96%), 1,3-hexadiene (Aldrich, 95%, mixture of (Z) and (E) isomers), and 3-methyl-1,3-pentadiene (Aldrich, 98%, mixture of (Z) and (E) isomers) were refluxed over calcium hydride for 3 h, then distilled trap-to-trap and stored under dry nitrogen. $CoCl_2(PRPh_2)_2$ (R = Me, Cy) were prepared as reported in literature [20,21,31].

4.2. Synthesis of Cobalt Complexes

4.2.1. Synthesis of $(\eta^3\text{-}C_4H_7)(\eta^4\text{-}C_4H_6)Co(PCyPh_2)$ (**1**)

The cobalt complex $CoCl_2(PCyPh_2)_2$ (2.53 g, 3.82 mmol) was introduced in a 100 mL round-bottomed Schlenk flask. Ethanol (3 mL), and a solution of 1,3-butadiene (12.4 mL, 159 mmol) in heptane (13 mL) were then added. The solution so obtained was cooled at −30 °C, and zinc powder (3 g, 45.9 mmol) was finally added. The suspension was kept under stirring at −30 °C for one day, then at −10 °C for one day, at 0 °C for a further day, and finally at +20 °C for a couple of days. The color of the final suspension was green, but the supernatant solution appeared red after decanting. The suspension was filtered, the red filtrate slightly concentrated under vacuum, and then cooled to −30 °C. After three days at low temperature, red single crystals, suitable for X-ray analysis, were formed, which were separated and dried under vacuum at room temperature. Yield: 0.80 g (47.9% based on $CoCl_2$). NMR and X-ray characterization of the complex is reported in the text.

4.2.2. Synthesis of $(\eta^3\text{-}C_4H_7)(\eta^4\text{-}C_4H_6)Co(PMePh_2)$ (**2**)

The cobalt complex $CoCl_2(PMePh_2)_2$ (2.89 g, 5.4 mmol) was introduced in a 100 mL round-bottomed Schlenk flask. Ethanol (3 mL), and a solution of butadiene (17 mL, 220 mmol) in heptane (17 mL) was then added. The solution so obtained was cooled at −30 °C, and the zinc powder (4.15 g, 63.5 mmol) was finally added. The suspension was kept at −30 °C under stirring for one day, then at 0 °C for one day and finally at +20 °C for a further day. The color of the suspension changed from blue to green to orange–yellow to the final red. After three days, the suspension was filtered; the filtrate was transferred in a refrigerator at −25 °C and kept at this temperature for three days. Red crystals of **2**, unfortunately not suitable for X-ray molecular structure determination, were formed, which were separated from the solution and dried under vacuum. Yield: 1.06 g (53.4% based on $CoCl_2$). NMR of the complex is reported in the text.

4.2.3. Synthesis of $(\eta^3\text{-}C_5H_9)(\eta^4\text{-}C_5H_8)Co(PMePh_2)$ (**3**)

The cobalt complex $CoCl_2(PMePh_2)_2$ (2.85 g, 5.4 mmol) was introduced in a 100 mL round-bottomed Schlenk flask. Ethanol (3 mL), heptane (17 mL) and isoprene (21.5 mL, 215 mmol) were then added. The solution so obtained was cooled at −30 °C, and zinc powder (4.17 g, 63.7 mmol) was finally added. The suspension was kept under stirring at −30 °C for one day, then at −10 °C for one day, and finally at +20 °C for one day. The color of the final suspension was red. The suspension was filtered, the red filtrate slightly concentrated under vacuum, and then cooled to −30 °C. No crystals were formed after three days; the solvent was indeed removed under vacuum, and pentane was added on the residue. The solution was filtered, and then kept at low temperature for crystallization. After one week, no precipitate was formed; the solvent was again removed under vacuum obtaining a highly viscous red oil as a residue which was dried under vacuum. Yield: 3.59 g (81.6% based on $CoCl_2$). NMR of the complex is reported in the text.

4.3. Cobalt Complexes Characterization

4.3.1. X-ray Crystallographic Studies of (η^3-C_4H_7)(η^4-C_4H_6)Co($PCyPh_2$) (**1**)

A summary of the experimental details concerning the X-ray diffraction study of complex **1** is reported in Tables 1 and S1. The intensity data were collected on a Bruker Smart Apex CCD area detector (Bruker AXS Inc., Madison, WI, USA) using graphite-monochromated Mo Kα radiation (λ = 0.71073 Å). Data reduction was made with SAINT and absorption corrections based on multiscan were obtained by SADABS [32]. The structure was solved by SHELXS-97 [33] and refined on F2 by full-matrix least-squares using SHELXL-14 [34]. All the non-hydrogen atoms were refined anisotropically. Hydrogen atoms were placed in calculated positions and included in the refinement as 'riding', excepted those bonded to the η^3 (C1–C3) and η^4 (C5–C8) coordinated carbon atoms. The H isotropic thermal parameters were fixed at 1.2 (1.5 for methyl groups) times the equivalent thermal parameter of the atoms to which they are bonded. The program ORTEPIII was used for graphics [35]. Crystallographic data were deposited with the Cambridge Crystallographic Data Centre as supplementary publication no. CCDC 1585813. These data can be obtained free of charge via www.ccdc.cam.ac.uk/conts/retrieving.html (or from CCDC, 12 Union Road, Cambridge CB2 1EZ, UK; fax: +44-1223-336-033; e-mail: deposit@ccdc.cam.ac.uk).

4.3.2. Computational Details

Geometry optimization of isolated, gas phase complexes (η^3-C_4H_7)(η^4-C_4H_6)Co($PRPh_2$) with R = cyclohexyl, phenyl and methyl were performed by the Gaussian16 program package [36], using the 6–311 g(d) basis set and the M06 functional, due to its specific parametrization on organometallic complexes [37]. The X-ray molecular structure of the complex with R = cyclohexyl was used as starting point for geometry optimization of all compounds, after the required atoms substitutions, owing to the lack of either the structure for the complex with R = methyl or the Cartesian coordinates of the deposited structure for the complex with R = phenyl [16].

4.3.3. NMR Characterization

^{1}H and 2D experiments were acquired on Bruker DMX 500 spectrometer, and on Bruker Avance 400 (Bruker Italia S.r.l., Milano, Italy). Samples were dissolved in hexadeuterobenzene, at 25 °C and were internally referred to the ^{1}H signal of residual benzene. The ^{1}H NMR conditions were the following: 5 mm probe; 8.75 μs as 90° pulse, relaxation delay 3 s; acquisition time 2.72 s. TOCSY (TOtal Correlation SpectroscopY) experiments correlate protons that interact through J-couplings showing correlations between all protons within a given spin system. The experiments were performed using a standard pulse sequence, with a mixing time of 0.1 s; power level for tocsy spin-lock 12 dB; low power pulse 52.80 μs. ROESY (Rotating frame Overhauser Effect SpectroscopY) experiments allow to detect protons that are close to each other in the space, even if they are not bonded. Spectra were recorded in phase sensitive mode using a standard pulse sequence; power level for roesy spin-lock 20 dB; spin-lock pulse 200 ms.

4.4. Polymerization

All operations were carried out under an atmosphere of dry dinitrogen. A standard procedure is reported. 1,3-Butadiene was condensed into a 25 mL dried glass reactor kept at −20 °C, then toluene was added and the solution so obtained was brought to the desired polymerization temperature. The cobalt allyl compound was then added as toluene solution. The polymerization was terminated with methanol containing a small amount of hydrochloric acid; the polymer was coagulated and repeatedly washed with methanol, then dried in vacuum at room temperature to constant weight. MAO, when used, was added just before the introduction of the cobalt compound.

The polymerizations with the other monomers (i.e., 1,2 propadiene, isoprene, (*E*)-1,3-pentadiene, 1,3-hexadiene, 3-methyl-1,3-pentadiene) were carried out in the same way.

4.5. Polymer Characterization

^{13}C and ^{1}H NMR measurements were carried out on a Bruker AVANCE 400 spectrometer, operating at 400 MHz for ^{1}H and 100.58 MHz for ^{13}C. The spectra were obtained in $C_2D_2Cl_4$ at 103 °C (hexamethyldisiloxane, HMDS, as internal standard). The concentration of polymer solutions was about 10 wt %. ^{13}C NMR conditions were the following: 10 mm probe; 14.50 μs as 90° pulse, relaxation delay 18 s; acquisition time 1.87 s. Proton broad-band decoupling was achieved with a 1D sequence using bi_waltz_16_32 power-gated decoupling. DSC scans were carried out on a Perkin Elmer Pyris 1 Instrument (Perkin Elmer, Milano, Italy) equipped with a liquid nitrogen sub-ambient device. The sample, ca. 4 mg, was placed in a sealed aluminum pan and the measurements were carried out using heating and cooling rates of 20 °C/min. The molecular weight averages (M_w) and the molecular weight distribution (M_w/M_n) were obtained by a Waters GPCV 2000 system (Waters S.p.A., Milano, Italy) using two on-line detectors: a differential viscosimeter and a refractometer. The experimental conditions consisted of two PLgel Mixed C columns, *ortho*-dichlorobenzene as mobile phase, 0.8 mL/min of flow rate and 145 °C of temperature. The calibration of the GPC system was carried out using eighteen narrow M_w/M_n polystyrene standards with the molar weights ranging from 162 to 5.6×10^6 g/mol. X-ray powder diffraction profiles were obtained with Ni filtered CuKα radiation with an automatic diffractometer X-Pert by Panalytical (Panalytical, Almelo, The Netherlands).

5. Conclusions

Novel allyl cobalt phosphine complexes were synthesized, which were found to be able to polymerize 1,3-dienes and allene, exhibiting different activity and selectivity depending on the type of phosphine ligand coordinated to the metal atom and the type of monomer. The structures of these new allyl complexes, determined through NMR and X-ray techniques, and the structure of the polymers obtained, determined by NMR spectroscopy, provided further support and confirmation of the 1,3-dienes polymerization mechanism that has been proposed previously [18,22].

Supplementary Materials: The following are available online at www.mdpi.com/2073-4344/7/12/381/s1, Table S1: Crystallographic data and results of structure refinement for **1**. Figure S1: TOCSY NMR spectrum of **2**. Figure S2: TOCSY NMR spectrum of **3**. Figure S3: ROESY NMR spectrum of **3**. Figure S4: ROESY NMR spectrum of **2**. This material is available free of charge via the Internet at http://sciencedirect.com.

Author Contributions: Giovanni Ricci conceived and designed the experiments, performed the organometallic syntheses, interpreted the results and wrote the paper. Giuseppe Leone performed the organometallic syntheses and the polymerizations. Antonella Caterina Boccia performed the NMR characterization of the cobalt complexes and contributed to write the paper. Alessandra Forni determined the X-ray molecular structures of the complexes, performed the quantum-mechanical calculations and contributed to write the paper.

Conflicts of Interest: The authors declare no conflict of interest.

References

1. Porri, L.; Giarrusso, A. Part II: Conjugated Diene Polymerization. In *Comprehensive Polymer Science*; Pergamon: Oxford, UK, 1989; Volume 4, pp. 53–108.
2. Thiele, S.K.H.; Wilson, D.R. Alternate Transition Metal Complex Based Diene Polymerization. *J. Macromol. Sci.* **2003**, *C43*, 581–628. [CrossRef]
3. Osakada, K.; Takeuchi, D. Coordination Polymerization of Dienes, Allenes, and Methylenecycloalkanes. *Adv. Polym. Sci.* **2004**, *171*, 137–194.
4. Friebe, L.; Nuyken, O.; Obrecht, W. Neodymium-Based Ziegler/Natta Catalysts and their Application in Diene Polymerization. *Adv. Polym. Sci.* **2006**, *204*, 1–154.
5. Dagorne, S.; Fliedel, C. Organoaluminum species in homogeneous polymerization catalysis. *Top. Organomet. Chem.* **2013**, *41*, 125–172.

6. Wilke, G.; Bogdanovic, B.; Hardt, P.; Heimbach, P.; Keim, W.; Kromer, M.; Oberkirch, W.; Tanaka, K.; Steinrucke, E.; Walter, D.; et al. Allyl-Transition Metal Systems. *Angew. Chem. Int. Ed. Engl.* **1966**, *5*, 151–164. [CrossRef]
7. Porri, L.; Natta, G.; Gallazzi, M.C. Polymerization of butadiene and cycloolefins by π-allylnickel bromide. *Chim. Ind. (Milan)* **1964**, *46*, 428–429, (*Chem. Abstr.* **1964**, *61*, 1944).
8. Shmonina, V.L.; Stefanovskaya, N.N.; Tinyakova, E.I.; Dolgoplosk, B.A. Stereospecific polymerization of dienes catalyzed by π-allyl complexes of chromium on aluminosilicate. *Vysokomol. Soedin. Ser. B* **1970**, *12*, 566.
9. Teyssie, P.; Dawans, F. π-Allyl-type polymerization. *Ind. Eng. Chem. Prod. Res. Dev.* **1971**, *10*, 261–269.
10. Dolgoplosk, B.A.; Tinyakova, E.I. Nature of active centers and mechanism of coordination polymerization. I. Nature of active centers during the stereospecific polymerization of dienes and mechanism of stereoregulation. *Vysokomol. Soedin. Ser. A* **1977**, *19*, 2441–2463.
11. Ashitaka, H.; Ishikawa, H.; Ueno, H.; Nagasaka, A. Syndiotactic 1,2-polybutadiene with Co-CS_2 catalyst system. I. Preparation, properties, and application of highly crystalline syndiotactic 1,2-polybutadiene. *J. Polym. Sci. Polym. Chem. Ed.* **1983**, *21*, 1853–1860. [CrossRef]
12. Ashitaka, H.; Jinda, K.; Ueno, H. Syndiotactic 1,2-polybutadiene with Co-CS_2 catalyst system. II. Catalysts for stereospecific polymerization of butadiene to syndiotactic 1,2-polybutadiene. *J. Polym. Sci. Polym. Chem. Ed.* **1983**, *21*, 1951–1972. [CrossRef]
13. Ashitaka, H.; Inaishi, K.; Ueno, H. Syndiotactic 1,2-polybutadiene with Co-CS_2 catalyst system. III. ^{1}H- and ^{13}C-NMR study of highly syndiotactic 1,2-polybutadiene. *J. Polym. Sci. Polym. Chem. Ed.* **1983**, *21*, 1973–1988. [CrossRef]
14. Ashitaka, H.; Jinda, K.; Ueno, H. Syndiotactic 1,2-polybutadiene with Co-CS_2 catalyst system. IV. Mechanism of syndiotactic polymerization of butadiene with cobalt compounds–organoaluminum–CS_2. *J. Polym. Sci. Polym. Chem. Ed.* **1983**, *21*, 1989–1995. [CrossRef]
15. Ricci, G.; Italia, S.; Porri, L. Polymerization of butadiene to 1,2-syndiotactic polymer with (η^5-C_8H_{13})(η^4-C_4H_6)Co. Some observations on the factors that determine the stereospecificity. *Polym. Commun.* **1988**, *29*, 305–307.
16. Porri, L.; Vitulli, G.; Zocchi, M.; Allegra, G. A but-2-enyl-buta-1,3-diene complex of cobalt. *J. Chem. Soc. D* **1969**, *6*, 276–277. [CrossRef]
17. Vitulli, G.; Porri, L.; Segre, A.L. Preparation and Properties of a But-2-enyl Butadiene Complex of Cobalt and of an Analogous Complex from Isoprene. *J. Chem. Soc. A* **1971**, 3246–3250. [CrossRef]
18. Ricci, G.; Sommazzi, A.; Masi, F.; Ricci, M.; Boglia, A.; Leone, G. Well Defined Transition Metal Complexes with Phosphorus and Nitrogen Ligands for 1,3-Dienes Polymerization. *Coord. Chem. Rev.* **2010**, *254*, 661–676. [CrossRef]
19. Ricci, G.; Leone, G.; Boglia, A.; Boccia, A.C.; Zetta, L. *cis*-1,4-*alt*-3,4 Polyisoprene: Synthesis and Characterization. *Macromolecules* **2009**, *42*, 9263–9267. [CrossRef]
20. Ricci, G.; Forni, A.; Boglia, A.; Motta, T.; Zannoni, G.; Canetti, M.; Bertini, F. Synthesis and X-ray Structure of $CoCl_2(P^iPrPh_2)_2$. A New Highly Active and Stereospecific Catalyst for 1,2 Polymerization of Conjugated Dienes When Used in Association with MAO. *Macromolecules* **2005**, *38*, 1064–1070. [CrossRef]
21. Ricci, G.; Forni, A.; Boglia, A.; Sommazzi, A.; Masi, F. Synthesis, structure and butadiene polymerization behavior of $CoCl_2(PR_xPh_{3-x})_2$ (R = methyl, ethyl, propyl, allyl, isopropyl, cyclohexyl; x = 1, 2). Influence of the phosphorous ligand on polymerization stereoselectivity. *J. Org. Chem.* **2005**, *690*, 1845–1854. [CrossRef]
22. Porri, L.; Giarrusso, A.; Ricci, G. Recent views on the mechanism of diolefin polymerization with transition metal initiator systems. *Prog. Polym. Sci.* **1991**, *16*, 405–441. [CrossRef]
23. Ricci, G.; Battistella, M.; Porri, L. Chemoselectivity and Stereospecificity of Chromium(II) Catalysts for 1,3-Diene Polymerization. *Macromolecules* **2001**, *34*, 5766–5769. [CrossRef]
24. Ricci, G.; Morganti, D.; Sommazzi, A.; Santi, R.; Masi, F. Polymerization of 1,3-dienes with iron complexes based catalysts. Influence of the ligand on catalyst activity and stereospecificity. *J. Mol. Catal. A Chem.* **2003**, *204/205*, 287–293. [CrossRef]
25. Ricci, G.; Forni, A.; Boglia, A.; Sonzogni, M. New Chromium(II) Bidentate Phosphine Complexes: Synthesis, Characterization, and Behavior in the Polymerization of 1,3-Butadiene. *Organometallics* **2004**, *23*, 3727–3732. [CrossRef]
26. Ricci, G.; Forni, A.; Boglia, A.; Motta, T. Synthesis, structure, and butadiene polymerization behavior of alkylphosphine cobalt(II) complexes. *J. Mol. Catal. A Chem.* **2005**, *226*, 235–241. [CrossRef]

27. Ricci, G.; Boglia, A.; Motta, T. Synthesis of new Cr(II) complexes with bidentate phosphine ligands and their behavior in the polymerization of butadiene. Influence of the phosphine bite angle on catalyst activity and stereoselectivity. *J. Mol. Catal. A Chem.* **2007**, *267*, 102–107. [CrossRef]
28. Ricci, G.; Leone, G.; Boglia, A.; Bertini, F.; Boccia, A.C.; Zetta, L. Synthesis and Characterization of Isotactic 1,2-Poly(*E*-3-methyl-1,3-pentadiene). Some Remarks about the Influence of Monomer Structure on Polymerization Stereoselectivity. *Macromolecules* **2009**, *42*, 3048–3056. [CrossRef]
29. Boccia, A.C.; Leone, G.; Boglia, A.; Ricci, G. Novel stereoregular *cis*-1,4 and *trans*-1,2 poly(diene)s: Synthesis, characterization, and mechanistic considerations. *Polymer* **2013**, *54*, 3492–3503. [CrossRef]
30. Ricci, G.; Leone, G. Recent progresses in the polymerization of butadiene over the last decade. *Polyolefins J.* **2014**, *1*, 43–60.
31. Chatt, J.; Shaw, B.L. Alkyls and aryls of transition metals. Part IV. Cobalt(II) and iron(II) derivatives. *J. Chem. Soc.* **1961**, 285–290. [CrossRef]
32. Bruker. *SMART, SAINT and SADABS*; Bruker AXS Inc.: Madison, WI, USA, 1997.
33. Sheldrick, G.M. A short history of SHELX. *Acta Cryst.* **2008**, *A64*, 112–122. [CrossRef] [PubMed]
34. Sheldrick, G.M. Crystal structure refinement with SHELXL. *Acta Cryst.* **2015**, *C71*, 3–8.
35. Burnett, M.N.; Johnson, C.K. *ORTEP-III: Oak Ridge Thermal Ellipsoid Plot Program for Crystal Structure Illustrations*; Oak Ridge National Laboratory Report ORNL-6895; Oak Ridge National Laboratory: Oak Ridge, TN, USA, 1996.
36. Frisch, M.J.; Trucks, G.W.; Schlegel, H.B.; Scuseria, G.E.; Robb, M.A.; Cheeseman, J.R.; Montgomery, J.A., Jr.; Vreven, T.; Kudin, K.N.; Burant, J.C. *Gaussian 16, Revision A.03*; Gaussian, Inc.: Wallingford, CT, USA, 2016.
37. Zhao, Y.; Truhlar, D.G. The Mo6 suite of density functionals for main group thermochemistry, thermochemical kinetics, noncovalent interactions, excited states, and transition elements: Two new functionals and systematic testing of four Mo6-class functionals and 12 other functionals. *Theor. Chem. Acc.* **2008**, *120*, 215–241.